

# MODELLING AND DYNAMIC SIMULATION OF A REAL CRUDE OIL OFFSHORE PLANT USING ASPEN HYSYS®

Damian, R.\*; Sotelo, C.\*#; Marroquin, J.\*; Cruz, E.\*\* & Sotelo, D.\*

\* Tecnológico de Monterrey, Escuela de Ingeniería y Ciencias, Ave. Eugenio Garza Sada 2501 Sur, Col: Tecnológico, 64700 Monterrey, N.L., México

\*\* Pemex, Exploración y Producción, Ciudad del Carmen, Mexico

E-Mail: a01384428@tec.mx, carlos.sotelo@tec.mx, a01570807@exatec.tec.mx, ezequiel.cruz@pemex.com, david.sotelo@tec.mx (# Corresponding author)

## Abstract

In the offshore crude oil process, water separation has a significant impact on quality improvement. Moreover, the lower the oil content in the residual stream, the less treatment is needed to fulfil specifications. Herein, the use of simulation has become an important tool to achieve a better understanding of the process. However, considering that the petrochemical plant is subjected to extreme time varying operating conditions, which affects the separation train; this poses a challenge to obtain a realistic simulation model. This work presents our original dynamic simulation of a complete crude oil separation unit using Aspen HYSYS® environment. The inlet feed is characterised as a heavy crude oil and different pieces of equipment are carefully designed according to real process parameters. Furthermore, the impact on variations in water content and irregular flows, known as slug flow occurrence, is analysed. Finally, to validate the accuracy of the simulation, operating temperatures, pressures for the separators, and the main flows of the process are compared with actual data.

(Received in November 2025, accepted in January 2026. This paper was with the authors 2 weeks for 1 revision.)

**Key Words:** Oil-Water-Gas Separation, Heavy Oil, Dynamic Simulation, Slug Flow, Aspen HYSYS®

## 1. INTRODUCTION

Offshore oil production occurs in isolated environments, leading to complex and extreme operating conditions [1, 2]. After the crude oil extraction process is carried out, petroleum contains significant amounts of gas and water causing corrosion and operational issues in the pipelines [3]. Therefore, to obtain a high-quality product, suitable for transportation and refining process, a proper three-phase separation is required [4]. Herein, modelling and simulation play a key role to achieve a better understanding of the process [5, 6]. Steady state modelling and simulation for petrochemical plants are commonly encountered in literature [7, 8]. Al-Ali [9] presents a crude oil stabilisation process simulation, with an analysis on input variables and a resulting modified process. Additionally, Cho et al. [10] present a steady state simulation of a conceptual design of a top-side process of an offshore oil processing plant, comparing its production with the original design. Nguyen et al. [11] provide a steady state model of three platforms located in the North Sea, with a focus on energy analysis. As it can be seen, most of the reported models are primarily developed in steady state, capturing the fundamental behaviour of multiphase flow during regular operation. Nevertheless, petrochemical units do not operate in steady state, which implies that these models are of limited usefulness [4, 7]. Therefore, to establish a real-time monitoring system, dynamic models for processing plants are required. Khaled et al. [2], provide a methodology for building a process model, generating a simulation based on a real petrochemical plant in the North Sea, considering equipment faults and inlet disturbances to simulate safety and continuous operation [12]. Moreover, Jonach et al. [13] present a simulation of an offshore oil and gas separation process with a focus on the transient behaviour of oil residues in output water. However, most simulations are simplified and do not take into account complex

dynamics present during routine operations. For this reason, the present research work provides a rigorous dynamic simulation model of an offshore oil separation process developed using Aspen HYSYS<sup>®</sup>. Here, two main stages are involved: the oil conditioning unit and the three phase treatment stage. The full details of the plant equipment are set according to the design data from a Mexican conventional offshore oil processing plant. Additionally, the inlet stream of the oil process is simulated considering composition variations and irregular flows, known as slug flow occurrence. Thus, a complete and realistic plant under recurrent operational problems during production is carried out.

## 2. SYSTEM DESCRIPTION

Fig. 1 shows the diagram of the offshore crude oil plant. The process consists of two main stages. The first stage corresponds to the conditioning unit, in which the gas and water contents in the inlet flow are decreased by biphasic and liquid-liquid separators. Meanwhile, in the second stage a three phase separator is used to obtain a high quality petroleum.

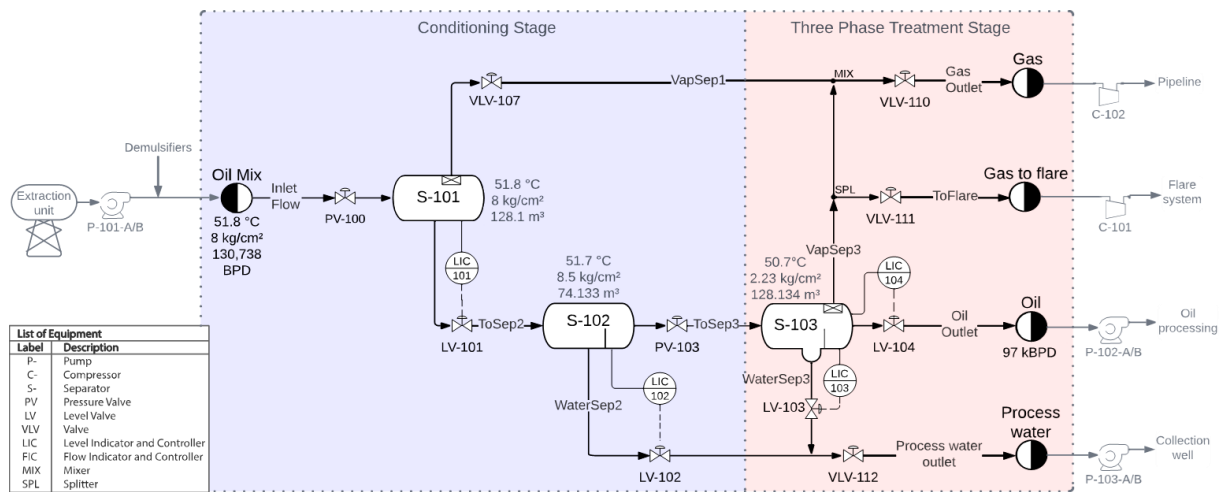


Figure 1: Flow diagram of the separation plant.

In the conditioning unit, 130 thousand barrels per day (MBPD) of liquid and 27 million cubic feet per day (MMCFD) of gas feed the process. Before the mixture is sent to the two phase liquid-gas separator S-101, the pressure is regulated to 755.1 kPa by the valve PV-100. Moreover, the liquid level in the separator is regulated at 1800 mm by controller LIC-101. Then, the gas from the stream is reduced to 3.5 MMCFD and the removed gas is conducted to a pipeline for its long-distance transportation. Meanwhile, the remaining liquid proceeds to the liquid-liquid separator S-102, in which the controller LIC-102 is set to regulate the liquid level at 914 mm. Here, the water content from the stream is removed by gravimetric settling and directed to a collection well. Thus, 114 MBPD of liquid are sent to the next stage.

In the three phase treatment stage, the separator S-103 is used to remove impurities from the stream. The pressure of the inlet feed is regulated by valve PV-103 to 117.7 kPa. Moreover, controller LIC-103 regulates the water liquid level in the first chamber at 600 mm, while controller LIC-104 regulates the oil liquid level in the second chamber at 1652 mm. Therefore, 97 MBPD of dehydrated high-quality oil outlet is obtained.

## 3. SIMULATION AND MODELLING

In Fig. 2, the simulation of the process is conducted using the Aspen HYSYS<sup>®</sup> environment, which is recognised in a wide range of oil, gas and petrochemical applications [14]. The use of this engineering tool in complex separation processes provides accurate results to the actual

plant conditions [15, 16]. Moreover, the software offers dynamic modelling capabilities that integrate rigorous thermodynamic models with mathematical operations to represent system behaviour and predict thermophysical properties of complex mixtures [17].

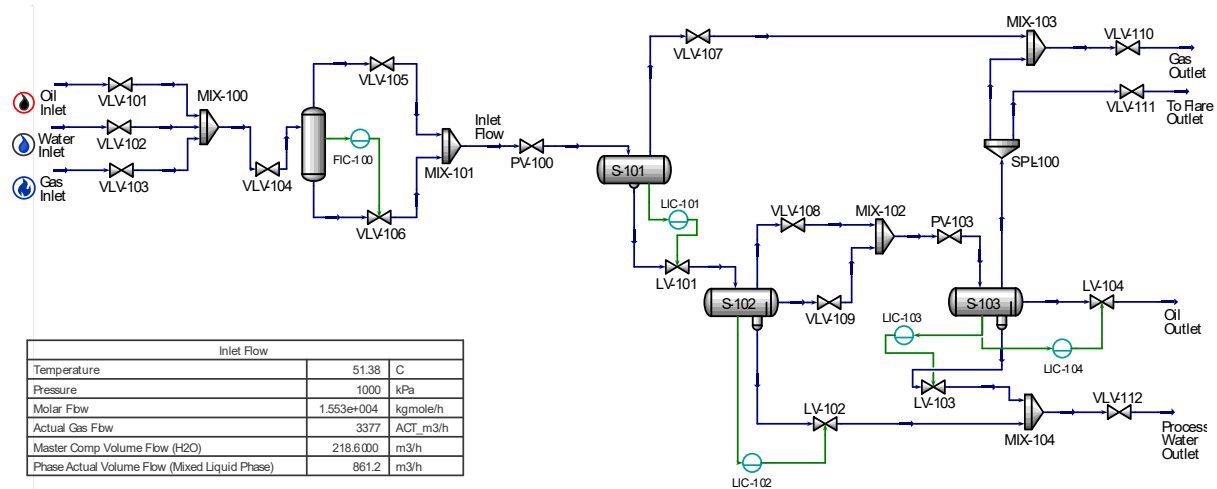


Figure 2: Aspen HYSYS® process flow diagram.

Here, the Equation of State (EoS) from the Peng-Robinson fluid package is selected. Hence, simulations in steady-state and dynamic modes are carried out, especially the gravity separators, which are part of the most important equipment in the upstream petroleum industry [18]. The simulation of these units is based on their operating principles, configured either as a two-phase separator for gas-liquid (Fig. 3 a) and liquid-liquid (Fig. 3 b) separation, or as a three-phase separator, for output streams separation (Fig. 3 c).

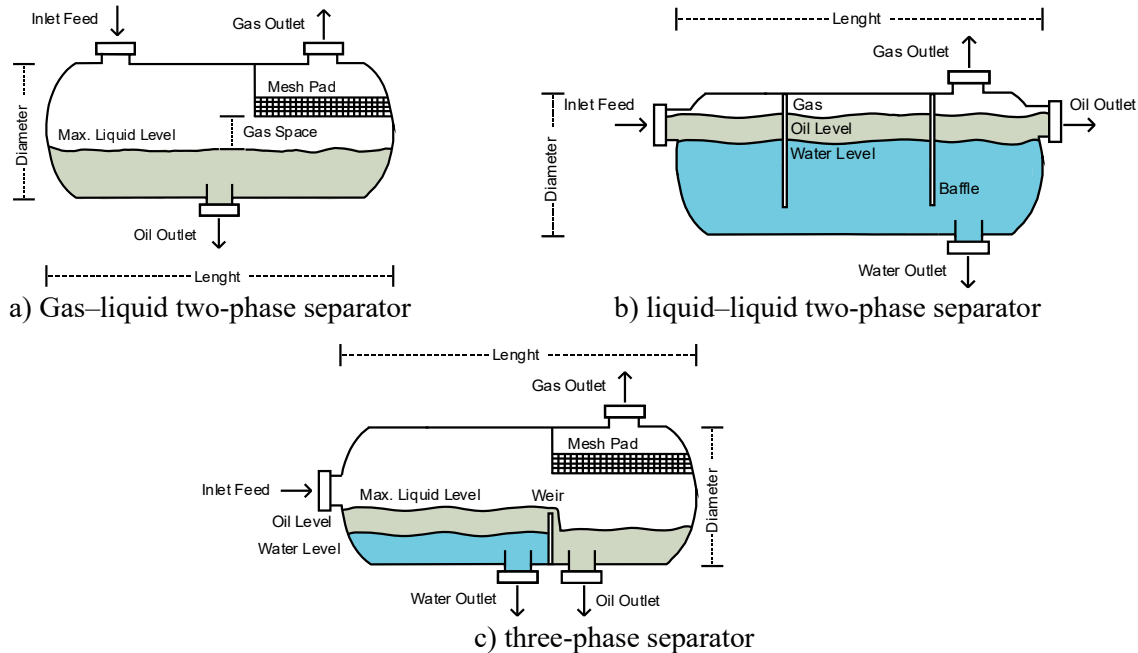


Figure 3: Gravity separators used in the simulation.

### 3.1 Oil characterisation

Crude oil characterisation is crucial for the design of separation equipment, since important fluid properties influence the settling behaviour of dispersed phases in gravity-based separators [19]. To provide the input feed for the separation plant, a characterised heavy crude oil from the Gulf of Mexico is used, whose general properties are described by

Seidy-Esfahlan et al. [20]. The composition used in simulation is based on Table I, which presents data from an actual chromatography of the process.

Table I: Inlet composition data.

Component ID	Molar fraction in oil inlet	Component ID	Molar fraction in oil inlet
Methane	0.196	CO <sub>2</sub>	0.00273
Ethane	0.0489	H <sub>2</sub> S	0.000236
Propane	0.0441	M-Cyclopentane	0.00232
i-Butane	0.0125	Benzene	0.000036
n-Butane	0.04	Cyclohexane	0.00139
i-Pentane	0.0177	M-Cyclohexane	0.000135
n-Pentane	0.0233	Toluene	0.00067
n-Hexane	0.0518	Styrene	0.0000756
n-Heptane	0.00178	m-Xylene	0.0000126
n-Octane	0.00216	p-Xylene	0.0000126
n-Nonane	0.00319	o-Xylene	0.000841
Nitrogen	0.00494	Maya1-Maya27	0.5456

### 3.2 Steady state

According to actual data, in this section the separators for the conditioning and three phase treatment stages are modelled in steady state using Aspen HYSYS<sup>®</sup>. Here, to enhance water-oil emulsion separation, the units S-102 and S-103 units are simulated as horizontal three-phase separators [21], both operating at approximately 52 °C and within the same pressure range. Additionally, operating at a lower temperature and pressure, 51.38 °C and 1000 kPa, the unit S-101 is designed as a horizontal biphasic separator to direct the volatile components in the mixture to the gas stream.

A pressure–temperature (PT) phase diagram was developed to evaluate the thermodynamic behaviour of the main streams, Fig. 4. Phase envelopes were generated for the inlet feed and the output streams from each separator, representing the saturation boundaries at different qualities. The feed shows the widest two-phase region and highest critical pressure. As lighter components are progressively removed, the phase envelope shifts to lower pressures and decreases in height, corresponding to S-101, S-102, and S-103. The red, blue, and grey curves represent the envelopes for the feed and the sequential separation stages, illustrating the expected reduction of the two-phase region and critical pressure, consistent with steady-state operation.

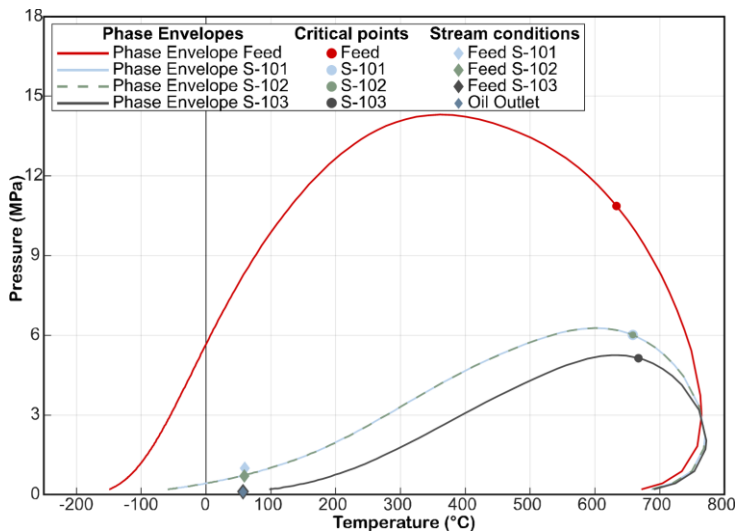


Figure 4: Phase diagram envelope.

### 3.3 Dynamic state

To set up the dynamic model, the same input load from steady-state simulation is used, consisting of an oil flow of 0.178 m<sup>3</sup>/s, a water flow of 0.0607 m<sup>3</sup>/s, and a standard gas flow (measured at standard conditions of 15 °C and 101.3 kPa) of 102.0196 m<sup>3</sup>/s. Additionally, the equipment sizing and geometric parameters for separators, including volume, diameter, weir specifications, are carefully defined in Table II. Also, the corresponding dynamic nozzle locations, are carefully defined. Specifically, for vessel S-101, the vapour outlet nozzle is positioned at 10.16 m, whereas for vessel S-103, the vapour, oil, and water outlet nozzles are located at 9.14 m, 12.19 m, and 4.06 m, respectively, with a weir height of 2.3 m and a weir located at 6.095 m along the vessel length. The mesh pads in the separators were modelled using the Carpenter method, with a pad thickness of 0.305 m, wire diameter of 0.000406 m, voidage of 0.5, and specific surface area of 377.3 m<sup>2</sup>/m<sup>3</sup>. These size and geometric parameters are required to enable CarryOver Correlation, which is used to simulate imperfect separation of phases based on a specified model [22]. For the purpose of this research, vessels S-101 and S-103 use ProSeparator Correlation while S-102 uses Product Basis Correlation to better represent the behaviour of a liquid-liquid separator based on design data. Moreover, valves are set up according to design data and to comply with Aspen HYSYS<sup>®</sup> dynamic flow requirements. The valve sizing is done by Aspen HYSYS<sup>®</sup> and level controllers are set up, according to Khaled et al. [2], for the vessels based on design data objectives.

Table II: Geometric parameters of separators.

Equipment	Volume (m <sup>3</sup> )	Diameter (m)	Length (m)	Light liquid level (m)	Heavy liquid level (m)
S-101	128.1	3.658	12.19	1.8	1.8
S-102	74.13	3.048	10.16	-	-
S-103	128.1	3.658	12.19	1.652	0.6

## 4. SIMULATION PROCEDURE

In this section, the equations used to obtain the vapour-liquid equilibrium (VLE), which is based on the Peng-Robinson EOS, are presented.

### 4.1 Vapour-liquid equilibrium equations

Eq. (1) expresses the equality of chemical potential between the phases for component  $i$  in a multicomponent system, where  $P$  represents the system pressure,  $\Phi_i^L$  and  $\Phi_i^V$  are the fugacity coefficients in the liquid and vapour phases, respectively, and  $x_i$  and  $y_i$  are the corresponding mole fractions:

$$P\Phi_i^L x_i = P\Phi_i^V y_i \quad (1)$$

The overall material balance is given by Eq. (2), where  $z_i$  represents the mole fraction of component  $i$  in the feed, while  $L$  and  $V$  correspond to the total molar flows of the liquid and vapour phases, respectively:

$$z_i F = x_i L + y_i V \quad (2)$$

The distribution coefficients are defined as the ratio between the fugacity coefficients in both phases, Eq. (3):

$$K_i = \Phi_i^L / \Phi_i^V \quad (3)$$

The summation of mole fractions equals unity in both phases, providing the closure condition for composition calculations.

## 4.2 Peng-Robinson EOS

The model relies on thermodynamic property estimation of each component in the fluid stream and is used to predict phase behaviour according to the Peng-Robinson EOS. This model is selected due to its extensive applicability in gas-liquid systems and its demonstrated capability to precisely predict the phase behaviour associated with hydrocarbon mixtures, Eqs. (4) to (7) [23-26].

$$P = \frac{RT}{v-b} - \frac{a}{v(v+b) + b(v-b)} \quad (4)$$

In Eq. (4), the pressure  $P$  is determined as a function of the molar volume of the mixture  $v$  and is further influenced by  $a$  and  $b$ , which represent the attraction parameters of the components. Then,  $R$  denotes the universal gas constant, while  $T$  is the absolute temperature. In Eqs. (5) to (7),  $b$  is calculated as the weighted sum of the covolumes  $b_i$  of each component based on their molar fraction  $x_i$ , while  $a$  accounts for intermolecular interactions through  $a_{ij}$ , which depends on  $a_i$ ,  $a_j$ , and the binary interaction coefficient  $k_{ij}$ .

$$b = \sum_{i=1}^N x_i b_i \quad (5)$$

$$a = \sum_{i=1}^N \sum_{j=1}^N x_i x_j a_{ij} \quad (6)$$

$$a_{ij} = \sqrt{a_i a_j} (1 - k_{ij}) \quad (7)$$

The parameter  $a_i$  is obtained from the critical properties coefficient  $a_c$  and the temperature-dependent factor  $(1 - \sqrt{(T/T_c)})$ , while  $b_i$  is derived from the critical temperature and pressure, Eqs. (8) and (9). The terms  $a_c$  and  $m$ , the last one as a function of acentric factor  $\omega$ , are calculated according to Eqs. (10) and (11):

$$a_i = a_c [1 + m (1 - \sqrt{(T/T_c)})]^2 \quad (8)$$

$$b_i = 0.077796074 R T_c / P_c \quad (9)$$

$$a_c = 0.45723553 R^2 T_c^2 / P_c \quad (10)$$

$$m = 0.37464 + 1.54226\omega - 0.26992\omega^2 \quad (11)$$

The Peng–Robinson EOS is expressed in terms of the compressibility factor  $Z$  to simplify the analysis of volumetric and phase equilibrium properties under non-ideal conditions:

$$f(Z) = Z^3 + (B - 1) Z^2 + (A - 2B - 3B^2) Z + (B^3 + B^2 - AB) = 0 \quad (12)$$

Thermodynamic parameters  $A$  and  $B$  are derived from molecular interaction constants and system properties, Eqs. (13) to (15):

$$A = aP/(RT)^2 \quad (13)$$

$$B = bP/(RT) \quad (14)$$

$$Z = Pv/(RT) \quad (15)$$

Finally, using the logarithmic equation is obtained the fugacity coefficient  $\Phi_i$ , Eq. (16), where  $x_j$  can be substituted with  $y_j$  to represent either the liquid or gas mole fraction, according on the phase that is being computed.

$$\ln \Phi_i = \frac{b_i}{b} (Z - 1) - \ln(Z - B) - \left( \frac{A}{2\sqrt{2}B} \right) \times \left( \frac{2\sum_j x_j a_{ij}}{a} - \frac{b_i}{b} \right) \ln \left( \frac{Z+2.414B}{Z-0.414B} \right) \quad (16)$$

### 4.3 Methodology

Considering the VLE is performed in Aspen HYSYS<sup>®</sup>, using equilibrium calculations and the Peng-Robinson EOS to determine phase behaviour, the following methodology is proposed:

1. Set the input parameters of the mixture specified in Table I. Obtain the acentric factor  $\omega$  from component properties and define binary interaction parameter  $k_{ij}$  for each pair of components.
2. Establish pressure, temperature, size and volume for each piece of equipment specified in Table II. These values are set according to the resulting VLE equations from Aspen HYSYS<sup>®</sup>.
3. Obtain the VLE using Eq. (1) to Eq. (3). The coefficient  $K_i$  is obtained through the Peng-Robinson EOS.
4. Calculate the compressibility factor  $Z$  using Eq. (12). All the parameters used to obtain  $Z$  are the result of using Eq. (13) to Eq. (15).
5. Obtain the fugacity coefficient  $i$  for both phases using Eq. (16).
6. Compute the gas and liquid phase compositions in the mixture through the, now completed, VLE.
7. Iterate from step 3, with the calculated phase compositions, until convergence is achieved.
8. Calculate the outlet flow based on composition of phases.

## 5. SIMULATION RESULTS

To validate the model, temperatures, pressures and flows of main streams are compared with actual data from a conventional offshore plant. In addition, the performance of the simulation under real operating conditions is analysed when input load disturbances are encountered.

### 5.1 Steady state results

Separation efficiency analysis is crucial to understand how the system responds to parameter variations under real operating conditions [27]. Hence, in Table III, the validation data of steady state modelling is presented. Here, a small variation in the pressure for S-102 is encountered due to the use of a three-phase separator modelling instead of a liquid-liquid separator; however, the remain parameters are close to actual data.

Table III: Validation results for separation units and process.

Equipment	Liquid rate (MBPD)		Water rate (MBPD)		Gas rate (MMSCFD)		Temperature (°C)		Pressure (kPa)	
	Real	Sim	Real	Sim	Real	Sim	Real	Sim	Real	Sim
S-101	130	129.44	-	-	27	27.01	51.8	51.02	784.5	784.5
S-102	114	113.23	16	16.17	-	-	51.7	51.02	833.6	735.5
S-103	97	94.39	17	17.03	3.5	3.42	50.7	49.48	117.7	117.7
Overall process outlet	97	94.36	33	33.21	30.5	30.42	-	-	-	-

### 5.2 Dynamic simulation results

Actual data is analysed to establish maximum and minimum input load variations in water content and intermittent flow. Variations in water load and the implementation of slug flow are simulated using the arrangement shown in Fig. 5. Here, inlet water variations are applied

by the manipulation of the control valve VLV-101 based on disturbances shown in Table IV. Moreover, slug flow is modelled using a biphasic separator and a valve arrangement with an intermittent reintegration of gas and liquid streams occurring at a 1 mHz frequency [28]. This behaviour is reproduced through a manual flow disturbance introduced by the control valve VLV-103, operated using the FIC-100 controller in manual mode, which directly sets the valve position to emulate periodic slugs.

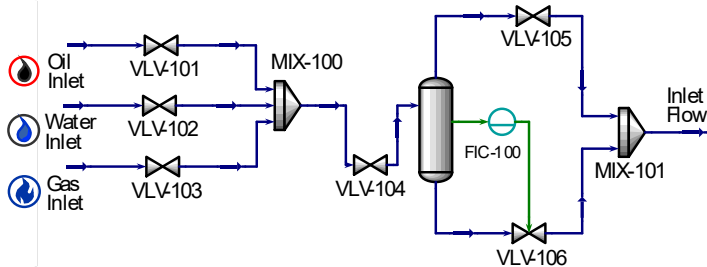


Figure 5: Input disturbances arrangement.

Table IV: Water inlet disturbances.

Disturbances	Input	Flow rates (m <sup>3</sup> /s)
Water inlet	+38 %	0.0607 → 0.0841
	-28 %	0.0607 → 0.0437

Furthermore, a comparison of the dynamic requirements of the units is presented in Table V. As it can be seen, both the diameter based in heuristics [29] and the real liquid level values, from the reported data [30], are close to the values in simulations. Herein, S-103 (1) and S-103 (2) refer to the internal chambers of the three-phase separator, corresponding to Chamber 1 and Chamber 2, respectively.

Table V: Dynamic requirements of the units.

Equipment	Diameter (m)		Liquid level (m)	
	Sim	Heuristics	Sim	Real
S-101	3.658	3.625	1.800	1.800
S-102	3.048	-	0.914	0.914
S-103 (1)	3.658	3.463	0.600	0.600
S-103 (2)	3.658	3.463	1.652	1.652

In Fig. 6 the effects of the disturbances in the input load are presented. Initially, only changes on water flow at the input of the system are considered. Therefore, after 8.5 hours, slug flow is applied. This to analyse the influence of input load variations of intermittent flow on the system. Furthermore, the water separated by S-102 and S-103 is shown, as well as the oil produced, to evaluate separation efficiency.

During the first 8.5 hours of the simulation, the aqueous phase level in separator S-102 responds gradually to feed water fluctuations, while oil production remains stable, showing that the system can handle moderate disturbances without performance degradation. After 8.5 hours, with intermittent flow, more pronounced fluctuations occur in the aqueous phase of S-102 and S-103, along with increased oscillations in oil output, indicating inefficiencies under severe flow variations despite minimal impact on overall system performance.

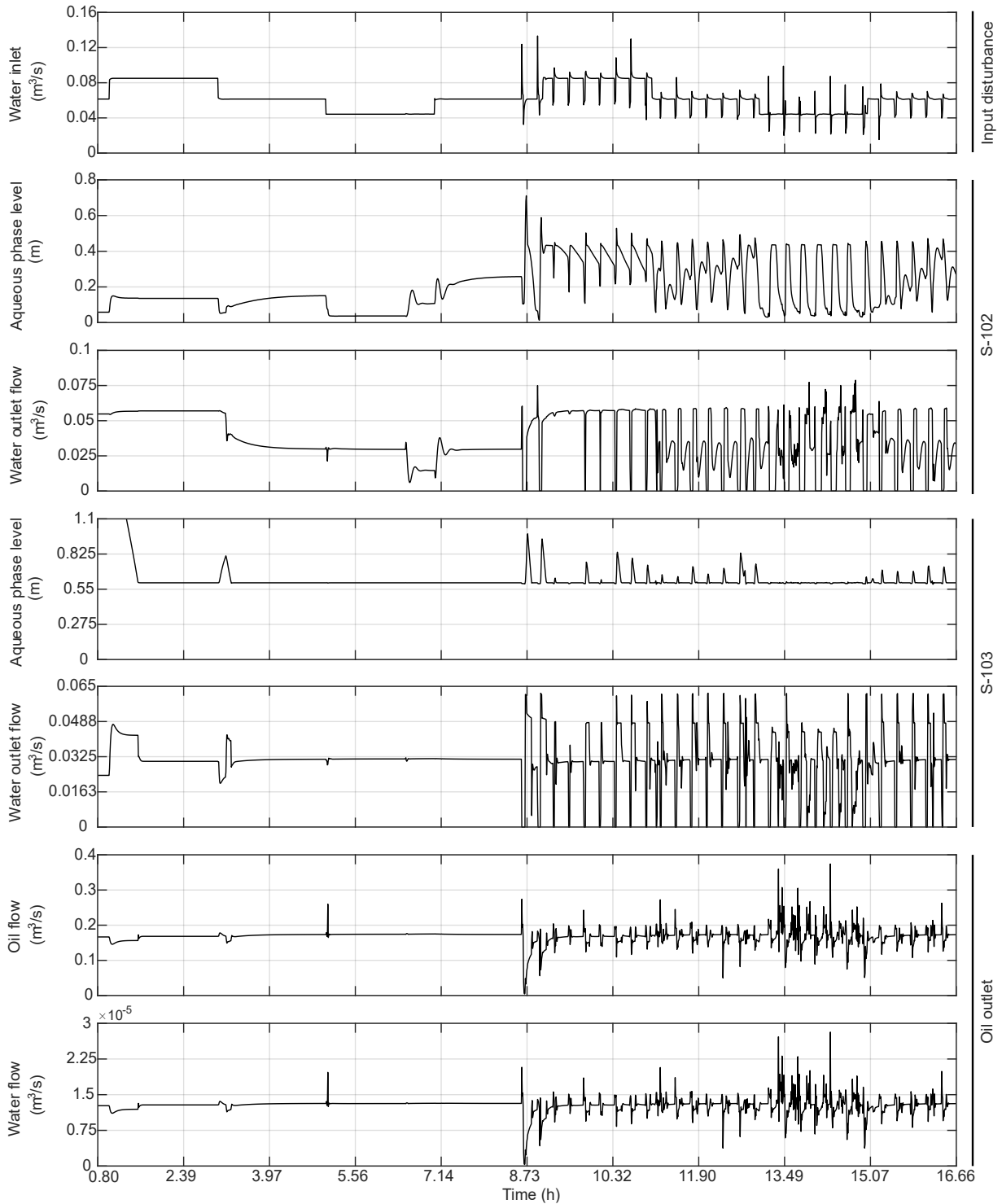


Figure 6: Water feed/composition and slug flow impact on water separation and oil production.

In Fig. 7, pressure distributions of each separator are shown. A significantly lower dispersion rate of pressure values is presented when slug flow is absent and displays intensified pressure oscillations as slug flow is introduced. Table VI, presents the maximum and minimum pressures, including its maximum rates. Here, the S-102 separator in the conditioning stage, exhibits the highest transient pressure fluctuations under both disturbance scenarios. Such instability reduces downstream reliability, creates a risk of mechanical damage [31, 32], and accelerates equipment degradation through slug-induced corrosion, which threatens the integrity of components and piping lines [33]. In addition, periods without

liquid inflow followed by high liquid rates also cause poor separation, low production, flooding, and, in severe cases, emergency shutdowns [34].

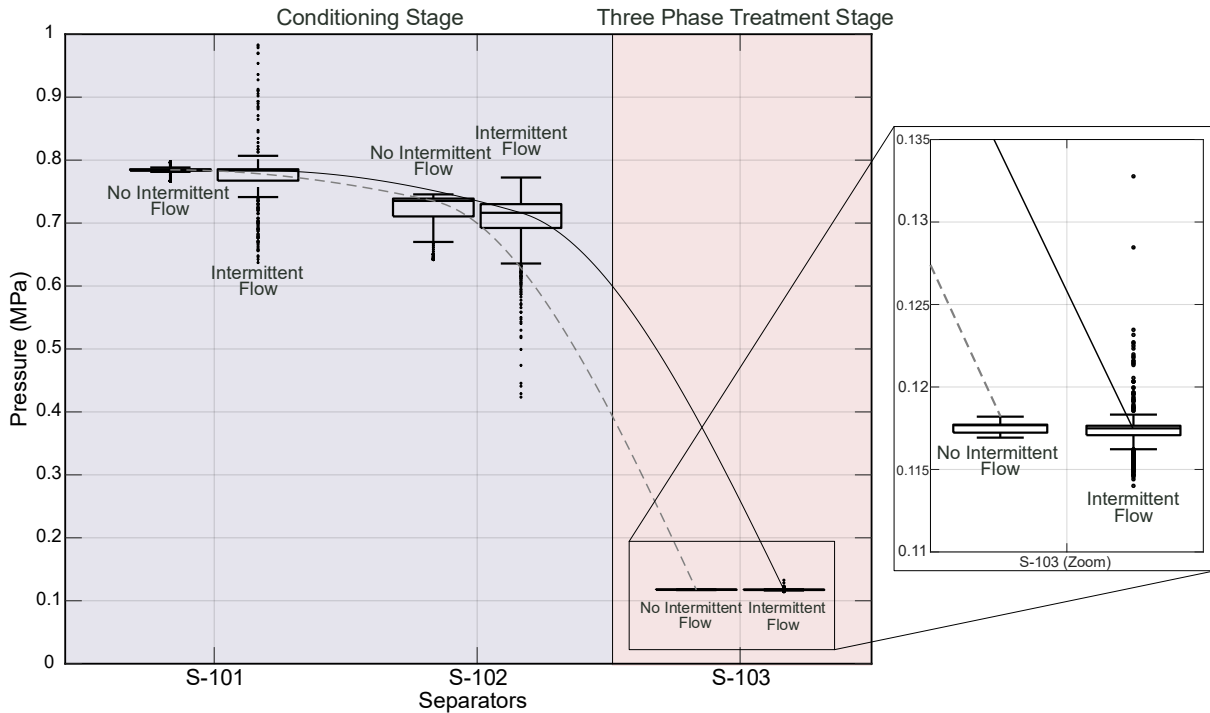


Figure 7: Boxplots and pressure variation through separators.

Table VI: Operating pressure range through separators.

Pressure values	No intermittent flow			Intermittent flow		
	S-101	S-102	S-103	S-101	S-102	S-103
Max	0.798	0.746	0.118	0.983	0.772	0.133
Min	0.767	0.642	0.117	0.637	0.424	0.114
Max variation	0.0196	0.104	0.0005	0.201	0.269	0.0174

## 6. CONCLUSION

In this work, a methodology was developed for simulating a crude oil offshore plant using Aspen HYSYS® environment in dynamic mode. Here, the geometric parameters of separators are set according to real design data and literature. Moreover, pressure, temperature, and stream flow data is validated with actual design data to generate a realistic simulation. Thus, the simulation is a proper representation of the dynamic behaviour of the process. When real operating conditions are incorporated to the process, the simulation results show that water content variations and intermittent flow do not have a significant impact on oil production or quality; however, the presence of both disturbances result in significant flow oscillations that can lead to equipment degradation. This is significant because of the difficulty of maintaining offshore plants, as their location is difficult to access and could lead to an increase in maintenance costs.

Considering that large-scale series processes are not common in the upstream oil and gas industry, the present work serves as a scientific platform to integrate real operating conditions to an oil separation process or to develop advanced control strategies, in response to these disturbances, for future research.

## REFERENCES

- [1] Dai, J. M.; Zhu, H. M.; Dai, Z. X.; Chen, M.; Du, L. B. (2025). Simulation and optimization for oil and gas platform placement in mountainous regions, *International Journal of Simulation Modelling*, Vol. 24, No. 2, 297-308, doi:[10.2507/IJSIMM24-2-729](https://doi.org/10.2507/IJSIMM24-2-729)
- [2] Khaled, M. S.; Imtiaz, S.; Ahmed, S.; Zendejboudi, S. (2021). Dynamic simulation of offshore gas processing plant for normal and abnormal operations, *Chemical Engineering Science*, Vol. 230, Paper 116159, 17 pages, doi:[10.1016/j.ces.2020.116159](https://doi.org/10.1016/j.ces.2020.116159)
- [3] Da Silva, M.; Sad, C. M. S.; Pereira, L. B.; Corona, R. R. B.; Bassane, J. F. P.; dos Santos, F. D.; Neto, D. M. C.; Silva, S. R. C.; Castro, E. V. R.; Filgueiras, P. R. (2018). Study of the stability and homogeneity of water in oil emulsions of heavy oil, *Fuel*, Vol. 226, 278-285, doi:[10.1016/j.fuel.2018.04.011](https://doi.org/10.1016/j.fuel.2018.04.011)
- [4] Ali, A. A.; Abdul-Majeed, G. H.; Al-Sarkhi, A. (2025). Review of multiphase flow models in the petroleum engineering: classifications, simulator types, and applications, *Arabian Journal for Science and Engineering*, Vol. 50, No. 7, 4413-4456, doi:[10.1007/s13369-024-09302-0](https://doi.org/10.1007/s13369-024-09302-0)
- [5] Ozowe, W.; Daramola, G. O.; Ekemezie, I. O. (2024). Innovative approaches in enhanced oil recovery: a focus on gas injection synergies with other EOR methods, *Magna Scientia Advanced Research and Reviews*, Vol. 11, No. 1, 311-324, doi:[10.30574/msarr.2024.11.1.0095](https://doi.org/10.30574/msarr.2024.11.1.0095)
- [6] Alrabghi, A. (2025). A modelling approach for asset degradation: advancing digital twin in maintenance, *International Journal of Simulation Modelling*, Vol. 24, No. 1, 76-86, doi:[10.2507/IJSIMM24-1-715](https://doi.org/10.2507/IJSIMM24-1-715)
- [7] Sotelo, C.; Favela-Contreras, A.; Ramirez-Mendoza, R. A.; Beltran-Carbajal, F.; Cruz, E.; Sotelo, D. (2021). Rigorous dynamic simulation of a dehydration and desalting crude oil unit using Aspen HYSYS®, *International Journal of Simulation Modelling*, Vol. 20, No. 2, 231-242, doi:[10.2507/IJSIMM20-2-546](https://doi.org/10.2507/IJSIMM20-2-546)
- [8] Ahmed, I.; Iswara, A. P.; Abbas, S.; Jamal, F. Q.; Ahmad, I.; Shah, S. T. H.; Naseem, A. (2024). Modelling and optimization of an existing onshore gas gathering network using PIPESIM, *Heliyon*, Vol. 10, No. 15, Paper e35006, 14 pages, doi:[10.1016/j.heliyon.2024.e35006](https://doi.org/10.1016/j.heliyon.2024.e35006)
- [9] Al-Ali, H. (2021). Process simulation for crude oil stabilization by using Aspen Hysys, *Upstream Oil and Gas Technology*, Vol. 7, Paper 100039, 9 pages, doi:[10.1016/j.upstre.2021.100039](https://doi.org/10.1016/j.upstre.2021.100039)
- [10] Cho, Y.; Kwon, S.; Hwang, S. (2018). A new approach to developing a conceptual topside process design for an offshore platform, *Korean Journal of Chemical Engineering*, Vol. 35, No. 1, 20-33, doi:[10.1007/s11814-017-0258-z](https://doi.org/10.1007/s11814-017-0258-z)
- [11] Nguyen, T.-V.; Voldsund, M.; Breuhaus, P.; Elmegaard, B. (2016). Energy efficiency measures for offshore oil and gas platforms, *Energy*, Vol. 117, Part 2, 325-340, doi:[10.1016/j.energy.2016.03.061](https://doi.org/10.1016/j.energy.2016.03.061)
- [12] He, D. X. (2024). Fault prediction in high-efficiency petroleum machinery production, *International Journal of Simulation Modelling*, Vol. 23, No. 1, 184-195, doi:[10.2507/IJSIMM23-1-CO5](https://doi.org/10.2507/IJSIMM23-1-CO5)
- [13] Jonach, T.; Haddadi, B.; Jordan, C.; Harasek, M. (2023). Dynamic simulation of a gas and oil separation plant with focus on the water output quality, *Energies*, Vol. 16, No. 10, Paper 4111, 18 pages, doi:[10.3390/en16104111](https://doi.org/10.3390/en16104111)
- [14] Farahbod, F. (2024). Improvement of operating conditions and composition of streams in gas condensate stabilization unit with the aim of reducing flare gas in Sarkhon and Qeshm gas plant, *Journal of Petroleum Exploration and Production Technology*, Vol. 14, No. 2, 555-566, doi:[10.1007/s13202-023-01718-y](https://doi.org/10.1007/s13202-023-01718-y)
- [15] Olugbenga, A. G.; Al-Mhanna, N. M.; Yahya, M. D.; Afolabi, E. A.; Ola, M. K. (2021). Validation of the molar flow rates of oil and gas in three-phase separators using Aspen Hysys, *Processes*, Vol. 9, No. 2, Paper 327, 17 pages, doi:[10.3390/pr9020327](https://doi.org/10.3390/pr9020327)
- [16] Wang, Y.; Shang, D.; Yuan, X.; Xue, Y.; Sun, J. (2020). Modeling and simulation of reaction and fractionation systems for the industrial residue hydrotreating process, *Processes*, Vol. 8, No. 1, Paper 32, 19 pages, doi:[10.3390/pr8010032](https://doi.org/10.3390/pr8010032)
- [17] Gholamzadeh, E.; Ghaemi, A.; Shokri, A.; Heydari, B. (2025). Investigation of boiler energy consumption in the gas refinery units using RSM ANN and Aspen HYSYS, *Heliyon*, Vol. 11, No. 1, Paper e41450, 14 pages, doi:[10.1016/j.heliyon.2024.e41450](https://doi.org/10.1016/j.heliyon.2024.e41450)

- [18] Mokhatab, S.; Poe, W. A.; Mak, J. Y. (2019). Phase Separation (Ch. 5), *Handbook of Natural Gas Transmission and Processing: Principles and Practices*, 4<sup>th</sup> ed., Gulf Professional Publishing, Cambridge, 191-217
- [19] Huang, S.; He, X.; Chen, J.; Wang, X.; Zhang, J.; Dong, J.; Zhang, B. (2022). Study on the performance of an electric-field-enhanced oil-water separator in treating heavy oil with high water cut, *Journal of Marine Science and Engineering*, Vol. 10, No. 10, Paper 1516, 15 pages, doi:[10.3390/jmse10101516](https://doi.org/10.3390/jmse10101516)
- [20] Seidy-Esfahlan, M.; Tabatabaei-Nezhad, S. A.; Khodapanah, E. (2024). Comprehensive review of enhanced oil recovery strategies for heavy oil and bitumen reservoirs in various countries: global perspectives, challenges, and solutions, *Heliyon*, Vol. 10, No. 18, Paper e37826, 20 pages, doi:[10.1016/j.heliyon.2024.e37826](https://doi.org/10.1016/j.heliyon.2024.e37826)
- [21] Acharya, T.; Casimiro, L. (2020). Evaluation of flow characteristics in an onshore horizontal separator using computational fluid dynamics, *Journal of Ocean Engineering and Science*, Vol. 5, No. 3, 261-268, doi:[10.1016/j.joes.2019.11.005](https://doi.org/10.1016/j.joes.2019.11.005)
- [22] Sulaiman, F. A.; Sidiq, H.; Kader, R. (2024). Liquid carry-over control using three-phase horizontal smart separators in Khor Mor gas-condensate processing plant, *Journal of Petroleum Exploration and Production Technology*, Vol. 14, Nos. 8-9, 2413-2435, doi:[10.1007/s13202-024-01817-4](https://doi.org/10.1007/s13202-024-01817-4)
- [23] Pratt, R. M. (2001). Thermodynamic properties involving derivatives using the Peng-Robinson equation of state, *Chemical Engineering Education*, Vol. 35, No. 2, 112-115
- [24] Huang, D.; Yang, D. (2019). Improved enthalpy prediction of hydrocarbon fractions with a modified alpha function for the Peng-Robinson equation of state, *Fuel*, Vol. 255, Paper 115840, 15 pages, doi:[10.1016/j.fuel.2019.115840](https://doi.org/10.1016/j.fuel.2019.115840)
- [25] Peng, D.-Y.; Robinson, D. B. (1976). A new two-constant equation of state, *Industrial & Engineering Chemistry Fundamentals*, Vol. 15, No. 1, 59-64, doi:[10.1021/i160057a011](https://doi.org/10.1021/i160057a011)
- [26] Lopez-Echeverry, J. S.; Reif-Acherman, S.; Araujo-Lopez, E. (2017). Peng-Robinson equation of state: 40 years through cubics, *Fluid Phase Equilibria*, Vol. 447, 39-71, doi:[10.1016/j.fluid.2017.05.007](https://doi.org/10.1016/j.fluid.2017.05.007)
- [27] Song, S.; Liu, X.; Li, C.; Li, Z.; Zhang, S.; Wu, W.; Shi, B.; Kang, Q.; Wu, H.; Gong, J. (2023). Dynamic simulator for three-phase gravity separators in oil production facilities, *ACS Omega*, Vol. 8, No. 6, 6078-6089, doi:[10.1021/acsomega.2c08267](https://doi.org/10.1021/acsomega.2c08267)
- [28] Trentini, R.; Campos, A.; Salvador, M. A.; Scheuer, Y. M.; dos Santos, C. H. F. (2023). Unrestricted horizon predictive controller applied in a biphasic oil separator under periodic slug disturbances, *Processes*, Vol. 11, No. 3, Paper 928, 18 pages, doi:[10.3390/pr11030928](https://doi.org/10.3390/pr11030928)
- [29] Manning, F. S.; Thompson, R. E. (1995) *Oilfield Processing of Petroleum: Vol. 2 – Crude Oil*, PennWell Books, Tulsa
- [30] Petróleos Mexicanos – PEMEX, Exploración y Producción (2019). *Filosofía de Operación*, PEMEX, documento institucional, Ciudad de Mexico (in Spanish)
- [31] Wong, B.; McCann, J. A. (2021). Failure detection methods for pipeline networks: from acoustic sensing to cyber-physical systems, *Sensors*, Vol. 21, No. 15, Paper 4959, 83 pages, doi:[10.3390/s21154959](https://doi.org/10.3390/s21154959)
- [32] Windmeier, C.; Flegiel, F.; Döb, A.; Franz, R.; Schleicher, E.; Wiezorek, M.; Schubert, M.; Hampel, U. (2021). A new research infrastructure for investigating flow hydraulics and process equipment at critical fluid properties, *Chemie Ingenieur Technik*, Vol. 93, No. 7, 1119-1125, doi:[10.1002/cite.202000202](https://doi.org/10.1002/cite.202000202)
- [33] Shifler, D. A. (Ed.) (2022). *LaQue's Handbook of Marine Corrosion*, 2<sup>nd</sup> ed., John Wiley & Sons, Hoboken
- [34] Holagh, S. G.; Ahmed, W. H. (2024). Critical review of vertical gas-liquid slug flow: an insight to better understand flow hydrodynamics' effect on heat and mass transfer characteristics, *International Journal of Heat and Mass Transfer*, Vol. 225, Paper 125422, 69 pages, doi:[10.1016/j.ijheatmasstransfer.2024.125422](https://doi.org/10.1016/j.ijheatmasstransfer.2024.125422)